Competition for electrons favors N_2O reduction in denitrifying *Bradyrhizobium* isolates

Gao Y[1*], Mania D[1], Mousavi SA[2], Lycus P[1], Arntzen M[1], Woliy K[1†], Lindström K[2], Shapleigh JP[3], Bakken LR[1] and Frostegård Å[1*]

[1] Faculty of Chemistry, Biotechnology and Food Sciences, Norwegian University of Life Sciences, N-1432 Ås, Norway

[2] Ecosystems and Environment Research programme, Faculty of Biological and Environmental Sciences, and Helsinki Institute of Sustainability Science (HELSUS), University of Helsinki, Finland

[3] Department of Microbiology, Cornell University, Ithaca, New York, USA

[†]Present address: Department of Biology, Hawassa University, Hawassa, Ethiopia

[*]Corresponding authors

Abstract

The legume-rhizobium symbiosis accounts for the major part of the biological N_2 fixation in agricultural systems. Despite their lower need for synthetic nitrogen fertilizers, legume-cropped fields are responsible for substantial N_2O emissions. Several economically important legumes fix N_2 through symbiosis with bacteria belonging to the genus *Bradyrhizobium.* Many bradyrhizobia are also denitrifiers, and inoculation of legumes with N_2O-reducing strains has been suggested to mitigate N_2O emissions. Here, we analyzed the phylogeny and denitrification capacity of *Bradyrhizobium* strains, most of them isolated from peanut nodules. All performed at least partial denitrification, but only 37% were complete denitrifiers. This group shared a common phenotype with a strong preference for N_2O- over NO_3^--reduction. We tested if this could be due to low quantities of NO_3^- reductase (periplasmic Nap) but found that Nap was more abundant than N_2O reductase (Nos). This corroborates a recently proposed mechanism that the electron pathway from quinols to Nos via the cytochrome bc_1 complex outcompetes that to Nap via the membrane-bound NapC. We propose that this applies to all organisms which, like many bradyrhizobia, carry Nos and Nap but lack membrane-bond NO_3^- reductase (Nar). Supporting this, *Paracoccus denitrificans*, which has Nap and Nar, reduced N_2O and NO_3^- simultaneously.

Introduction

Emissions of nitrous oxide (N_2O), the third most important anthropogenic greenhouse gas, have been rising steadily during the past 150 years. Predictions for the rest of the century show either continued N_2O emission increases or rates of decrease slower than the decreases occurring in CO_2 emissions [1,2]. Agriculture is the main source of anthropogenic N_2O emissions, with denitrification playing the major role in most soils [3]. The primary cause of the emissions is excessive use of synthetic fertilizers [2,4], but cultivation of legumes also contributes substantially with a global average of 1.29 (range 0.03-7.09) kg N_2O-N ha^{-1} $year^{-1}$ while the corresponding estimate for fertilized agricultural fields was 3.22 (range 0.09-12.67) [5]. In both cases, the ultimate driver of the emission is input of reactive nitrogen which undergoes a series of redox reactions and eventually returns to the atmosphere as N_2O or N_2. Our aim should be to minimize the N_2O/N_2 emission ratio of the system [6]. To achieve this, novel mitigation options beyond "good agronomic practice" will be needed [7]. Several technical abatement options have been suggested, including precision fertilization and use of nitrification inhibitors [8].

An alternative strategy is to enhance the populations of N_2O reducing microorganisms in the soil. Selective *in situ* stimulation of N_2O reducing, indigenous soil organisms appears unrealistic, while some options for the addition of N_2O reducing microbes may be feasible. One is the suggestion to inoculate soybeans with rhizobia that are not only efficient N_2-fixers but also have the capacity to reduce N_2O [9-11]. At present, N_2O reduction is not taken into account when screening strains for their suitability as inoculants and, in fact, several of the commercial inoculants currently used are only partial denitrifiers [12]. For example, only one of the five *Bradyrhizobium* strains most commonly used as soybean inoculants in South America could reduce N_2O [13]. The growing global need for plant-based proteins is expected to require new areas to be used for legume cropping and will likely increase the demand for new legume varieties. Not all combinations of legume cultivar and rhizobial strain result in an efficient symbiosis [14,15]. Importantly, indigenous soil populations of rhizobia may not be compatible with a certain legume crop, especially if it has not been grown in that area before. Therefore, the expansion of legume cropping is creating an increasing demand for a wider variety of inoculants to ensure nodulation and optimal N_2 fixation efficacy [16]. This offers a golden opportunity to

mitigate N_2O emissions, providing that the inoculants are selected among rhizobial strains that can reduce N_2O.

The purpose of the present study was to determine how denitrification phenotypes vary across taxonomically diverse groups of bradyrhizobia, with particular focus on their capacity for N_2O reduction, and to understand cellular mechanisms that make these organisms potential sinks for N_2O. We determined the phylogenetic position of a set of *Bradyrhizobium* strains, obtained from different culture collections, and analyzed their capacity for denitrification. Most of the strains were isolated from nodules of peanut plants (*Arachis hypogaea*) growing in different regions of China. Peanut is the fourth most important legume crop globally, with China being the main producer [17]. We also included some bradyrhizobia from other parts of the world, isolated from peanut and other legumes.

Several taxonomic groups within the genus *Bradyrhizobium* have been reported to denitrify with many strains having truncated denitrification pathways lacking one or more of the steps [12, 18, 19]. A complete denitrification pathway in bradyrhizobia comprises the periplasmic reductase Nap for dissimilatory NO_3^- reduction, encoded as a part of the *napEDABC* operon; the Cu-containing nitrite reductase NirK encoded by *nirK* only or as a part of the *nirKV* operon, although cd_1-type NirS nitrite reductase has also been reported [20]; the cytochrome *c* dependent nitric oxide reductase cNor *(norCBQD* operon); and a clade I N_2O reductase Nos (*nosRZDYFLX* operon) [21-25]. While the bradyrhizobia along with a number of other denitrifiers, only have the periplasmic Nap for dissimilatory NO_3^- reduction, other denitrifiers have the membrane-bound Nar, or both. Nap is a periplasmic heterodimer (NapAB) consisting of the small electron transfer subunit NapB and the catalytic NapA, which draws electrons from quinol via the membrane-bound *c*-type tetrahaeme cytochrome NapC. Nar is a three-subunit enzyme (NarGHI) anchored in the membrane by NarI, which is a transmembrane protein that draws electrons from quinol to the catalytic NarG via NarH, both facing the cytoplasm [26, 27]. Nir, Nor and Nos receive electrons from the bc_1 complex via periplasmic small c-type cytochromes [28, 29]. Clade I type Nos reductase may in addition draw electrons from quinol via the membrane bound NosR [30].

In a recent study, Mania et al. [19] screened strains within the genus *Bradyrhizobium* for their denitrification phenotype. Most of them could perform two or more of the denitrification steps,

but only half of them could reduce N_2O. All the N_2O reducing strains displayed the same strong preference for N_2O over NO_3^- reduction when incubated under anoxic conditions, which was suggested to be due to competition between the electron pathways to Nap and Nos. The quantification of denitrification gene transcripts showed 5-8 times lower transcript numbers of *nap* compared to *nos,* however. Therefore, it could not be excluded that the phenomenon is due to low abundance of Nap compared to Nos. Here we have investigated the denitrification geno- and phenotypes for another set of bradyrhizobia and deepened our understanding of the competition for electrons between Nap and Nos by refined analyses of the electron flow kinetics in combination with the determination of the relative amounts of Nap and Nos by proteomics. In addition, we compared the denitrification kinetics of the bradyrhizobia with the denitrification model bacterium *Paracoccus denitrificans*, which holds a complete denitrification pathway including both Nap and Nar [26, 29]. The results showed that in all bradyrhizobia with complete denitrification, NO_3^- reduction was almost completely hampered in the presence of N_2O. The proteomics analysis provided evidence that this was not due to a low abundance of Nap. As expected, the NarG carrying *P. denitrificans* showed a different denitrification phenotype with simultaneous reduction of NO_3^- and N_2O.

Materials and methods

Bacterial strains and growth conditions

The rhizobial isolates were obtained from various culture collections. Table 1 shows a list of host plant and geographic origin of the strains used in the phylogenetic analysis (all listed isolates; details see [31-37]) and the strains analyzed for their denitrification capacity (all except the four strains from Ethiopia earlier determined to have a complete denitrification pathway [19]). Preparation of *Bradyrhizobium* cultures and growth conditions followed Mania et al. [19]. All cultures were grown at 28 °C in Yeast Mannitol Broth (YMB; [38]) (10 g l^{-1} D-mannitol, 0.5 g l^{-1} K_2HPO_4, 0.2 g l^{-1} $MgSO_4 \cdot 7H_2O$, 0.1 g l^{-1} NaCl and 0.5 g l^{-1} yeast extract; pH 7.0). The cultures were streaked for purity and single colonies were picked and checked for possible contaminating bacteria by sequencing of the 16S rRNA genes (see below). Single colonies were grown in YMB and were preserved in 15% (v/v) glycerol at -80 °C. For experiments involving gas kinetics and

proteomics, cultures were raised from the frozen stocks in stirred batches of 50 ml YMB supplemented with filter sterilized KNO_3 and/or KNO_2 solutions. The flasks were sealed with sterilized, gas tight butyl rubber septa (Matrix AS, Norway). Air was removed by applying vacuum for 6 x 360 s, followed by 30 s He-filling. The desired amount of O_2 and/or N_2O was injected into the headspace, and the over-pressure released [39]. Denitrification kinetics of *Bradyrhizobium* strains with complete denitrification pathways were compared to the model bacterium *Paracoccus denitrificans* PD1222, which was grown under the same conditions as the *Bradyrhizobium* strains, except that Sistrom´s medium supplemented with 2 mM KNO_3 was used [40,41].

Denitrification end products and gas kinetics analyses

Denitrification end-products were determined for all strains as described previously [42]. Detailed gas kinetics were measured following Mania et al. [19]. Pre-cultures were added to incubation vials (n=3) supplied with 1 mM initial KNO_3 and, when indicated, also with 0.5 mM KNO_2. Unless stated otherwise, 0.7 mL O_2 (1 vol% in headspace) and 0.7 ml N_2O (approximately 50 µmol N $vial^{-1}$) were added to the headspace at the start of the experiment (0 hpi, hours post inoculation). For the determination of end-products, the amounts of O_2, NO, N_2O and N_2 in the headspace were measured at the start and after 10 days of incubation.

All strains with a complete denitrification pathway according to the end-point analysis, as well as all HAMBI strains that had NO as end-product, were investigated further by analyzing gas kinetics in response to oxygen depletion. To secure an inoculum in which any previously synthesized denitrification enzymes had been diluted out by aerobic growth, all cultures were precultured aerobically for at least 6-8 generations. This was done in uncapped vials covered with aluminum foil (to allow oxygen transport), with vigorous stirring (600 rpm) at 28 °C. To further ensure the absence of hypoxia, the cultures were transferred to new vials before the OD_{600} reached 0.3. Portions of the precultures were inoculated into 120 ml vials containing 50 ml YMB supplemented with 1, 2 or 3 mM KNO_3 and with He, O_2 and N_2O in headspace as described above for the end-product measurements. The vials were placed in a robotized incubation system that frequently measured O_2, NO, N_2O and N_2 in headspace [39, 43]. Leakage and sampling losses were taken into account when calculating the rates of production/consumption of each gas, see

Molstad et al [39] for details. Earlier experiments determined that no gas production (NO, N_2O or N_2) took place from chemical reactions between of NO_2^- and the medium under the conditions used [19].

Nitrite and growth measurements

Samples for NO_2^- and growth measurements (0.1-1.0 ml) were taken manually from the liquid phase through the rubber septum of the vials using a sterile syringe. NO_2^- concentrations were determined immediately after each sampling by drawing a 10 µL liquid sample which was injected into a purging device containing 50% acetic acid with 1% (w/v) NaI (at room temperature), by which NO_2^- is reduced instantaneously to NO [44, 45]. The quantities of resultant NO were measured by chemiluminescence using a NO analyser (Sievers NOA™ 280i, GE Analytical Instruments). The system was calibrated by injecting standards. Sampling for NO_2^- measurements was done as frequently as the gas sampling from the *Bradyrhizobium* and *P. denitrificans* cultures.

Aerobic and anaerobic growth was investigated in detail for *Bradyrhizobium* sp. HAMBI 2125 to determine the growth yield per mol electrons transferred to O_2, N_2O, and to the entire denitrification pathway. Four treatments were compared: 1) 7% O_2 in headspace; 2) 0% O_2, 4 mM NO_3^-; 3) 0% O_2 and 10 ml N_2O; 4) 7% O_2, 4 mM NO_3^- and 10 ml N_2O. Pre-cultures were started from single colonies and grown in YMB under fully oxic conditions (21% O_2) for inoculation of the aerobic batch cultures (treatments 1 and 4), and under anoxic conditions for inoculation of the anaerobic batches (treatments 2 and 3). The OD_{600} of the aerobic pre-cultures was kept < 0.3 by regularly inoculating portions of the culture into vials with fresh medium. There were 6 replicate vials for each treatment. Liquid samples were taken from three of them every 6 h (0.85 ml) for growth measurements (OD_{600}). The three other replicates were only monitored for gas kinetics and were then used to measure final cell dry weight, to assess the growth yield per mol electrons to O_2 and N-oxides. To determine cell dry weight, entire culture volumes were centrifuged, washed twice in distilled water (resuspension and centrifugation), dried at 100 °C in Eppendorf tubes, and weighed. Cell numbers were determined by microscopic counts at selected sampling times, which gave a conversion factor of $5.8*10^8$ cells ml^{-1} * OD_{600}^{-1}. The estimated yield from

181 growth on O_2, N_2O and NO_3^- was 12.0, 8.5 and 6.7 E12 cells mol^{-1} electrons, respectively (Table
182 S1). The growth rates were 0.063, 0.031 and 0.024 h^{-1} for cells grown with O_2, N_2O and NO_3^-,
183 respectively (Fig. S1). The yields were used to calculate cell density throughout the incubations,
184 enabling the calculation of cell specific rates of electron flows to the various electron acceptors,
185 for details see Fig. S2 and Table S1.
186
187 *DNA extraction and gene sequence analyses*
188 Cultures were started from single colonies and incubated in YMB medium under oxic conditions
189 at 28 °C for five days. DNA was extracted using QIAamp DNA Mini Kit (Qiagen). Purity of the
190 strains was checked by Sanger sequencing of 16S rRNA amplicons (for primers and PCR conditions
191 see Table S2). The genome sequences were obtained from another ongoing project: (JGI Gold
192 study ID: Gs0134353), and their Genome accession numbers are listed in Table S3. Genome
193 sequences were analyzed using RAST (Rapid Annotations using Subsystems Technology). Whole-
194 genome average nucleotide identity (ANI) comparisons were done using FastANI v.0.1.2.
195 A phylogenetic tree that included all HAMBI and CCBAU strains from this study (Table 1), as
196 well as the Ethiopian strains AC70c, AC86d2, AC87j1 and AC101b and the type strain of all species
197 of the genus *Bradyrhizobium* (February 2020, http://www.bacterio.net/bradyrhizobium.html),
198 was constructed based on multilocus sequence analysis (MLSA) of the four housekeeping genes
199 *atpD* (ATP synthase F1, beta subunit), *glnII* (glutamine synthetase type II), *recA* (recombinase
200 A), *rpoB* (RNA polymerase, beta subunit). The sequences from all HAMBI strains used in the MLSA
201 analysis were obtained from the present study. Amplicons of *rpoB* and *atpD* of the Ethiopian
202 strains AC70c, AC86d2 and AC101b and *recA* from AC70c were Sanger sequenced. For primers
203 and PCR conditions, see Table S2. All other sequences were obtained from GenBank
204 (http://www.ncbi.nlm.nih.gov/genbank). The GeneBank accession numbers for all housekeeping
205 genes used are listed in Table S5. The gene sequences were aligned by ClustalW [46] in Bioedit
206 v7.0.5.3 [47], and the alignments were edited manually. The best-fit models of nucleotide
207 substitution were selected based on Akaike information criterion (AIC) applying MEGA7 [48].
208 The Bayesian phylogenetic analyses of the concatenated loci (*atpD-recA-glnII-rpoB*) of 78
209 *Bradyrhizobium* strains were performed using the algorithm Metropolis coupled Markov chain

Monte Carlo (MCMCMC) twice for ten million generations using MrBayes v3.2.7a program [49]. *Neorhizobium galegae* was used to root the tree. The general time reversible plus gamma distribution plus invariable sites (GTR + G + I) was chosen as the best-fit model of phylogenetic analyses of the four partition of the concatenated dataset (*atpD-glnII-recA-rpoB*). The algorithms were analyzed using Tracer v1.7 [50], and the phylogenetic trees were visualized by Figtree v1.4.3 (https://beast.community/figtree). For comparison with the MLSA tree based on four housekeeping genes, a phylogenetic tree of all the HAMBI test strains listed in Table 2 was constructed using the Genome Taxonomy Database Toolkit (GTDB-Tk) v0.3.2, which is based on a phylogeny inferred from the concatenation of 120 ubiquitous, single-copy proteins [51].

Proteomics

Relative quantification of the denitrification reductases was done for the strain *Bradyrhizobium* sp. HAMBI 2125, chosen as a representative for the complete denitrifiers (Fig. 1), which all showed the same preference for N_2O over NO_3^- reduction (Fig. 2A, S3, S4, S5). Cells were first raised from frozen stock under strictly aerobic conditions as explained above. As the aerobic preculture reached OD_{600} = 0.05 ($2.9*10^7$ cells ml^{-1}), it was used to inoculate 18 vials (1 ml inoculum $vial^{-1}$) containing YMB with 1 mM NO_3^- and with 1 ml N_2O (approximately 80 µmol N_2O-N $flask^{-1}$) and 1 % O_2 in headspace. Samples for protein analysis were taken i) from the aerobic inoculum; ii) just before transition to anaerobic respiration (22 hpi, when O_2 reached ~4.6 µM); iii) during the period of rapid reduction of exogenous N_2O (27 and 32 hpi); and iv) during the period of NO_3^- reduction to N_2 (36 hpi). Three replicate vials were harvested at each time point. Gas kinetics, NO_2^- concentrations and sampling times for proteomics are shown in Fig. S6. After measuring the OD_{600}, the samples were centrifuged (10 000 g, 4 °C, 10 min) and the cell pellets were stored at -20 °C for protein extraction. In addition, we harvested and froze cells from the aerobic preculture.

To extract the proteins, the cell pellets were thawed, resuspended in lysis buffer (20 mM Tris-HCl pH8, 0.1 % v/v Triton X-100, 200 mM NaCl, 1 mM DTT) and treated with 3x45 s bead beating with glass beads (particle size ⩽106 µm Sigma) at maximum power and cooling on ice between the cycles (MP Biomedicals™ FastPrep- 24™, Thermo Fischer Scientific Inc). Cell debris was

239 removed by centrifugation (10 000 g; 5 min) and the supernatant, containing water soluble
240 proteins, was used for proteomic analysis based on Orbitrap-MS as described before [52]. To
241 quantify the denitrification reductases we calculated the fraction of the individual enzymes as
242 percentages of the sum of all LFQ (label-free quantitation of proteins) abundances for each time
243 point.
244
245 **Results**
246 *Phylogenetic distribution of denitrifying bradyrhizobia*
247 The phylogenetic position of the 23 test strains was determined by MLSA analysis of four protein-
248 coding housekeeping genes (*atpD-glnII-recA-rpoB*) (Fig. 1). The analysis comprised 78
249 bradyrhizobial strains and included all hitherto described *Bradyrhizobium* reference species. All
250 but one of the 23 test strains listed in Table 1 were assigned to the *Bradyrhizobium japonicum*
251 supergroup (Fig. 1). The exception was *Bradyrhizobium lablabi* HAMBI 3052^T, which is a member
252 of the *Bradyrhizobium jicamae* supergroup according to the new genome-based taxonomy of
253 bradyrhizobia proposed by Avontuur et al. [53]. The test strains were placed in 11 lineages (clades
254 A-K) with high posterior probability (PP=1.00). Most test strains were clustered within the clades
255 of seven diverse bradyrhizobial species. Strains *Bradyrhizobium* sp. HAMBI 2134 and 2142 formed
256 a monophyletic cluster (clade G) with high posterior probability (1.00). *Bradyrhizobium* sp. strain
257 HAMBI 2116 was accommodated in a lineage (clade A) distant from other bradyrhizobia. The
258 phylogenetic relationships revealed by the four-gene MLSA tree (Fig. 1) were supported by the
259 results from an analysis of the HAMBI strains (listed in Table 2), based on the GTDB Tool kit (Fig.
260 S7). In both trees strains HAMBI 2299, 2153 and 2116 were most closely related to the reference
261 species *B. yuanmingense*; strains HAMBI 2125 (and 2126) and 2127 were closest to *B. ottawaense*;
262 strain HAMBI 2130 was closest to *B. shewense*; strains HAMBI 2115 was closest to *B. japonicum*
263 USDA6; strains HAMBI 2128 (as well as HAMBI 2129 and 2150, Table S4) were closest to *B.*
264 *arachidis*; strain HAMBI 3052 was closest to *B. lablabi.* Strains HAMBI 2149, 2133, 2136, 2137,
265 2151 and 2152 formed one cluster in the GTDB tree together with *B. japonicum* USDA 135. This
266 cluster was close to *B. liaoningense*, as also found in the MLSA analysis (Fig. 1), which did not

include *B. japonicum* USDA 135. Strains HAMBI 2134 (and 2135, Table S4) and 2142 formed a separate cluster in both trees.

We originally included 21 isolates from the HAMBI culture collection in our study, all deposited with different strain names. Pairwise whole genome comparisons revealed that some strains were very similar with ANI values >99.2% and in most cases >99.9 % (Table S4), which was also supported by the clustering of similar strains in the GTDB tree (Fig. S7). Since the strains within such clusters with ANI values >99% also showed practically identical denitrification phenotypes, we present the result for only one of the strains in each such cluster in the main paper, and the results for the others as supplementary information.

The denitrification end-product analysis showed that all test strains were denitrifiers, able to reduce NO_3^- and/or NO_2^- to NO, N_2O or N_2. Seven of the 19 strains tested for denitrification in the present study were complete denitrifers that reduced NO_3^- to N_2. The four Ethiopian strains AC87j1, AC86d2, AC101b and AC70c were determined earlier to be complete denitrifiers [19]. All complete denitrifiers except *B. lablabi* (clade K) belonged to the *B. japonicum* supergroup and were positioned in clades E, H, I and J. The clades E, H and J represented the species *B. guangxiense*, *B. ottawaense* and *B. shewense*, respectively. Clade I, accommodating strains *Bradyrhizobium* sp. HAMBI 2125 and AC70c, formed a separate, monophyletic group. The other test strains had truncated denitrification pathways and were able to reduce NO_3^- and NO_2^- to NO (5 strains) or N_2O (7 strains). The seven strains having N_2O as end-product were distributed in clades A, C, D and G. Three strains grouped with *B. arachidis* in clade C*. Bradyrhizobium* sp. strain HAMBI 2115 was placed in clade D along with *B. japonicum* USDA6^T. Three strains were accommodated in clades A and G, neither of which included any of the hitherto described *Bradyrhizobium* species. The strains with NO as denitrification end-product were found in clades B, C and F, which also harbored the species *B. yuanmingense*, *B. arachidis* and *B. liaoningense*, respectively. Strains HAMBI 2153 and 2149, as well as the strains highly similar to HAMBI 2149 (Table S4), were also examined using detailed gas kinetics to further examine whether they could reduce NO (Fig. S8). Like in the end-product investigation they produced large amounts of NO (14-15 µmol vial^{-1}) while no reduction of NO or N_2O was detected (Fig. S8).

Consistency between denitrification gene operons and end products

The genetic potential for denitrification, based on whole genome sequencing, and the corresponding phenotype, determined by end-point analysis and gas kinetics, were compared for 13 strains (Table 2), as well as for isolates with genomes with ANI values >99.2% to these strains (Table S4). The five strains able to reduce NO_3^- to N_2 had complete operons for all four reduction steps. For most of the other strains, with NO or N_2O as denitrification end -products, the lack of a function was explained by complete lack of the corresponding operon. However, two strains (HAMBI 2153 and HAMBI 2299) showed a discrepancy between denitrification genotype and phenotype. They were apparently unable to reduce NO and accumulated µM concentrations of NO, despite having the *nor* operon. Comparison of these strains with strains having functional NO reduction revealed that strain HAMBI 2153 had a frame shift in *norB*, while *norQ* was not in the correct reading frame. Strain HAMBI 2299 carried *nap, nir* and *nor* operons with all expected genes present. The end-point analysis of this strain showed that after 10 days of incubation with 1 mM NO_3^-, 0.5 mM NO_2^- and 1 ml N_2O in headspace, it had produced toxic levels (>10 µM) of NO. Inspection of the amino acid sequences did not reveal any obvious explanations for lack of Nor activity.

All N_2O-reducing Bradyrhizobium *strains preferred N_2O over NO_3^- as electron acceptor*

To determine if the complete denitrifiers identified in this study showed a similar, strong preference for N_2O over NO_3^- as reported by Mania et al. [19] for other *Bradyrhizobium* strains, detailed gas kinetics was analyzed. The results showed remarkably similar kinetics for all strains during and after the transition from aerobic to anaerobic respiration in vials to which N_2O had been added to the headspace (Figs. 2A, S3, S4, S5). Strain HAMBI 2125 was chosen as a representative for the complete denitrifiers. The NO_2^- concentration in cultures of this strain was measured along with the gas kinetics (Figs. 2A, S3), allowing the estimation of NO_3^- concentrations by N-mass balance.

The first phase, marked in blue, was dominated by O_2 respiration. When the O_2 concentration in the medium reached 4.6 µM, some NO_3^- reduction took place, measured as a slight accumulation of NO_2^- and NO (0.7 and 1.7 µmol; not clearly visible in the figure due to scaling).

The small but significant decrease in N_2O during the aerobic phase was caused by sampling losses, not by N_2O reduction or other reactions, as explained in Fig. S9. The same is seen for experiments presented in Figs. 2C and S3-S5. Reduction of exogenous N_2O started when the O_2 concentration in the liquid was approximately 3.0 µM and rapidly reached a rate of 10.4 ± 1.2 µmol N $flask^{-1}$ h^{-1}, matching the corresponding N_2 production rate of 9.7 ± 1.0 µmol N $flask^{-1}$ h^{-1}. This phase of rapid and stoichiometric reduction of N_2O to N_2, marked in pink, lasted until most of the exogenous N_2O was reduced. No NO_3^--reduction took place during reduction of the exogenous N_2O. When the exogenous N_2O was depleted, the rate of NO_3^- reduction increased and the rate of N_2 production decreased instantaneously to 2.22 ± 0.18 µmol $flask^{-1}$ h^{-1} (phase marked in green). When NO_3^- reduction started, the NO_2^- concentration increased sharply and reached approximately 200-350 µM (9.8-17.4 µmol $vial^{-1}$), accounting for 20-35% of the initial 50 µmol NO_3^--N. The N_2 curve for strain HAMBI 2125 reached a stable plateau at 123 µmol N_2-N, which accounts for the sum of N_2O- and NO_3-N present initially. The same experiment was conducted with other strains, but without measuring NO_2^- (Figs. S4, S5), and they all showed the same fast stoichiometric conversion of N_2O to N_2 and a subsequent slower production of N_2 from NO_3^-, lasting until the N_2O+NO_3^--N was completely recovered as N_2-N. Strain HAMBI 2125 showed good control of NO during the entire incubation period, reaching a small peak of 11 nmol $vial^{-1}$ (6.9 nM in the liquid) around 41 hpi. For the other strains NO concentrations never exceeded 50 nM, and most strains kept NO concentrations <20 nM during the entire incubation (Figs. 2A, S3, S4, S5).

Nar carrying Paracoccus denitrificans *showed no preference for N_2O over NO_3^-*

In accordance with our hypothesis, the Nar carrying *P. denitrificans* reduced NO_3^- simultaneously with the exogenously supplied N_2O, indicating no hampering of NO_3^- reduction by N_2O (Fig. 2C). In contrast to all the examined *Bradyrhizobium* strains (Figs. 2A, S3, S4, S5), *P. denitrificans* started to reduce NO_3^- and headspace N_2O concomitantly when the O_2 concentration was close to depletion and stoichiometrically accumulated NO_2^- from NO_3^- reduction. Nitrite reduction and emergence of NO started when most of the NO_3^- had been reduced to NO_2^-.

Electron flow rates

The rates of electron flow to the various reductases (fmol e^- $cell^{-1}$ h^{-1}) were calculated based on the measured gas- and NO_2^- kinetics. Since the growth yield per mol electron (to O_2 and nitrogen-oxides) was determined (Fig. S2 and Table S1), the cell density could be calculated for each time point throughout the incubation, based on the measured cumulated electron flow, thus enabling an estimation of cell specific electron flows throughout. In *Bradyrhizobium* strain HAMBI 2125 (Fig. 2B), the cell specific electron flow was sustained at a more or less constant level (5-6 fmol e^- $cell^{-1}$ h^{-1}) through the transition from respiring O_2 to respiring N_2O, until the external N_2O was depleted (phases marked blue and pink in the corresponding gas kinetics Fig. 2A), but declined to ~3-4 fmol e^- $cell^{-1}$ h^{-1} when depending on the activity of Nap. In *P. denitrificans* (Fig. 2D) there was instead a simultaneous electron delivery to Nar and Nos during the phase when exogenous N_2O was being reduced (marked pink in the corresponding gas kinetics, Fig. 2C). This was later followed by electron flow to Nir, Nor and Nos, after the depletion of nitrate. The cell specific respiratory metabolism was 10-13 fmol e^- $cell^{-1}$ h^{-1} during the phase dominated by aerobic respiration, then increased to approximately 15-16 fmol e^- $cell^{-1}$ h^{-1} when respiring NO_3^- and N_2O, followed by a decrease to approximately 8 fmol e^- $cell^{-1}$ h^{-1} during respiration of the accumulated NO_2^-.

Injection of N_2O to actively denitrifying cultures resulted in an immediate arrest of NO_3-reduction

To investigate whether the preferred electron flow to N_2O in the foregoing experiments could be explained by regulation at the transcriptional level (i.e. early expression of *nos*), N_2O was injected into a culture that was actively reducing NO_3^- to N_2. A transcriptional regulation would not result in an immediate switch to the exogenous N_2O as electron acceptor but would instead be seen as a simultaneous reduction of all N-oxides present. This was tested on strain HAMBI 2125 (Fig. 3). The cultures were incubated in vials containing YMB with 2 mM initial NO_3^-, and with 1% O_2 but without exogenous N_2O in the headspace. Denitrification (from NO_3^- reduction) commenced when O_2 reached 4.3 µM and proceeded at a rate of 2.6 ± 0.4 µmol N $flask^{-1}$ h^{-1}. At 32 hpi, when the cells were actively reducing NO_3^- to N_2, approximately 300 µmol N_2O-N was injected. This injection led to a complete suppression of NO_3^- reduction. The measured N_2 production rate was similar to the measured N_2O reduction rate (23.9 ±3.6 and 26.4 ±3.6 µmol N $flask^{-1}$ h^{-1},

383 respectively). NO accumulation during this phase declined rapidly to zero consistent with an
384 absence of NO_3^- reduction. The NO_3^- reduction recovered once the external N_2O was depleted,
385 as reflected by recovery of NO, and an N_2 production rate similar as that before the injection of
386 N_2O.

387 In an additional experiment, including all seven N_2O-reducing strains, exogenous N_2O was
388 present in the headspace from the start of the incubation (Fig. S5). As expected from the first
389 experiment (Fig. 2A), the exogenous N_2O was rapidly reduced, followed by slow production of N_2
390 from NO_3^- reduction. A second injection of N_2O into the actively denitrifying cultures resulted in
391 an immediate increase in the N_2 production rate, similar to that during reduction of the initial
392 N_2O. These results supported the notion that N_2O was preferred as electron acceptor over NO_3^-.
393
394 *The preference for N_2O over NO_3^- was not explained by the relative numbers of the different*
395 *reductases*
396 A proteomics analysis was done for strain HAMBI 2125. The abundance of NapA, NirK and NosZ
397 molecules, measured as intensities, were determined at different time points in cells sampled
398 during aerobic respiration (21% O_2), and during and after transition from 1% oxygen respiration
399 to denitrification (Fig. 4). The level of NorC molecules detected was two orders of magnitude
400 lower than those for the other reductases, suggesting that membrane-bound enzymes require a
401 different extraction protocol. Therefore, only values for the periplasmic reductases NapA, NirK
402 and NosZ were included here. The aerobic pre-incubation over several generations effectively
403 removed most of the old denitrification reductases, seen from the signals from NapA and NirK
404 being 293-585 times lower than those observed during denitrification. Nos values were only 16-
405 47 times lower, indicating low levels of constitutive transcription of the *nos* gene and translation
406 of the corresponding mRNA under aerobic conditions. All three reductases increased in
407 abundance during the O_2 depletion phase (blue) and when O_2 approached depletion, the
408 NapA/Nos and NapA/NirK ratios were 1.4±0.2 and 4.1±1.8 (sd, n=3). Interestingly, the NapA/Nos
409 ratio was stable during the period of strong respiration of exogenous N_2O, marked pink in Fig. 4,
410 with values of 1.5± 0.3 and 1.2 ± 0.2, although practically no NO_3^- reduction took place. The
411 NapA/Nos ratio decreased to 0.7 during the phase of NO_3^- reduction to N_2 (after depletion of

412 exogenous N_2O). A similar pattern was found for the NapA/NirK ratios, while the NosZ/NirK ratios
413 stayed around 1.0 during the anaerobic phase.
414
415 **Discussion**
416 The study comprised a set of taxonomically diverse *Bradyrhizobium* strains, as shown by the
417 phylogenetic tree (Figs. 1 and S7). This genus is commonly found among the most dominant
418 organisms in soil microbial communities [54,55] and of large environmental and economic value
419 for their N_2-fixation ability in symbiosis with legumes. Based on the MLSA analysis of four
420 concatenated housekeeping genes (Fig. 1) the strains clustered in eleven clades, covering various
421 parts of the phylogenetic tree. Five strains in three clades did not group with described
422 *Bradyrhizobium* species, suggesting that three new species may be delineated for these three
423 clades. Our results from the denitrification analyses support other studies showing that complete
424 denitrification pathways are more common in the *B. japonicum* supergroup than in other
425 phylogenetic branches of *Bradyrhizobium* [18,19]. The complete denitrifiers in the present study
426 belonged to clusters related to *B. shewense*, *B. ottawaense* and *B. guangxiense*, with the
427 exception of one strain which clustered with the distantly related *B. lablabi* (Fig. 1). Although this
428 suggests that some taxonomic groups of bradyrhizobia have higher frequency of complete
429 denitrifiers than others, taxonomic position cannot be used as an indicator of the denitrification
430 end-product since even very closely related strains may differ in this regard [19].
431 Recent research has revealed several transcriptional and post-transcriptional mechanisms
432 that influence the amounts of intermediate products released from denitrifying organisms [56-
433 60]. Although of value by itself, such information may be anecdotal. To understand the
434 environmental relevance of a regulatory mechanism, it is important to know how widespread it
435 is. We found the same preference for N_2O over NO_3^- as electron acceptor in all strains with
436 complete denitrification, as did Mania et al. [19] for a different set of isolates. This indicates a
437 phenomenon common to bradyrhizobia. In theory, it could be explained by lower numbers of
438 NapA molecules compared to NosZ molecules. The results by Mania et al. [19] for strain AC 87j1,
439 which is closely related to strain HAMBI 2125, could not disprove this, since transcription analysis
440 showed 5-8 times lower copy numbers of transcripts coding for NapA compared to NosZ. This

441 prompted us to perform a proteomics analysis in the present study. The results (Fig. 4) provided
442 clear evidence that the strong N_2O reduction was not due to higher abundance of NosZ *vs* NapA,
443 thus supporting the hypothesis by Mania et al. [19] that the electron pathway to NosZ is
444 inherently more competitive than that to NapA.

445 Electrons from the quinol pool are channeled to Nap via the membrane-bound NapC, and to
446 Nos, Nor and Nir via the membrane-bound bc_1 complex and periplasmic cytochromes [61]. Most
447 likely, the electron pathway to NosZ via bc_1 is inherently more competitive than that to NapAB
448 via NapC**,** plausibly due to a combination of stronger affinity for quinol and a higher k_{cat} of bc_1
449 versus NapC. This implies a general mechanism which may apply not only to bradyrhizobia, but
450 possibly to all denitrifiers that carry Nap and Nos but lack the membrane-bound Nar. Verifying
451 this will require testing of a wide range of organisms. As a first step, we included in this study a
452 comparison of the denitrification kinetics of the bradyrhizobia with *P. denitrificans*, which carries
453 Nar in addition to Nap and Nos. The results supported our hypothesis by clearly demonstrating
454 that, while the *Bradyrhizobium* strains left NO_3^- untouched as long as exogenously supplied N_2O
455 was present (Figs. 2A, S3, S4, S5), *P. denitrificans* reduced these electron acceptors
456 simultaneously (Fig. 2C). This suggests that the electron pathways from the quinol pool to NarG
457 via NarI and NarH and to NosZ via the bc_1 complex and cytochrome c compete equally well for
458 electrons, at least in *P. denitrificans*.

459 The proteomics analysis of HAMBI strain 2125 showed that NosZ was synthesized under fully
460 aeriated conditions, while NapA and NirK were not. Before sampling for proteomics analysis, the
461 cultures had been incubated in vials with vigorous stirring for at least 10 generations to secure
462 that denitrification reductases produced during earlier exposure to denitrifying conditions were
463 diluted to near extinction in the cells. This was the case for NapA and NirK in the sample from
464 21% O_2 (Fig. 4). NosZ molecules were, however, approximately 10 times more abundant than
465 NapA and NirK during this phase, which suggests constitutive, albeit low, synthesis of NosZ. The
466 transcription analysis of strain AC87j1 reported by Mania et al. [19] provides no clear explanation
467 to this, though. In the presence of 5 µM O_2 in the liquid, there were < 0.3 *nosZ* and *nirK* transcripts
468 $cell^{-1}$ with only slightly higher levels of *nosZ* than *nirK*. The *napA* transcription was somewhat
469 higher with 0.8 copies $cell^{-1}$. It is possible, still, that a low but steady production of Nos takes

place in these organisms irrespective of O_2 concentrations, in line with the higher β-galactosidase activity observed for a *nos-lacZ* fusion of *B. japonicum* compared to a *nap-lacZ* fusion [62, 63]. This could be a strategy for cells to be prepared for anaerobic conditions and avoid being entrapped in anoxia without energy to produce the denitrification machinery [56]. If so, it suggests that these bacteria may be ready to reduce any N_2O produced by other organisms in their environment, thus acting as net sinks for this greenhouse gas.

Seven strains lacked the last step of denitrification and thus had N_2O as end-product, explained by the absence of the entire *nos* operon in all cases (Table 2). When exposed to denitrifying conditions in the environment, such organisms will reduce all available N-oxides to N_2O and thus act as net producers of this greenhouse gas. Three strains had NO as denitrification end-product, but only HAMBI 2149 lacked the entire *nor* operon (Table 2). The other two strains, HAMBI 2153 and 2299, contained *nor* operons but showed some sequence differences compared to strains with functional NO reduction. Further investigations trying to elucidate the reason for the lacking NO reduction would, however, be beyond the scope of the present study. Organisms that produce NO but are incapable of reducing it are apparently not uncommon [19, 64, 65]. In the environment such organisms are most likely found in consortia with organisms that express Nor or other NO-reducing enzymes.

The estimated growth yields were calculated based on the electron flow to the different reductases (Table S1) and the proportions were expected to match that of the charge separations per electron transport for the various respiratory pathways, as listed by [66]. The number of charge separations per 10 electrons ($q/10e^-$) are 50 for low affinity oxidase, 40 for high affinity oxidases, 30 for Nos alone, and 26 for the entire Nap, Nir, Nor, Nos denitrification pathway (NO_3^- to N_2), which would a yield ratio of 100:60:52 for the three pathways (O_2, N_2O, $NO_3 \rightarrow N_2$) if we assume that low affinity oxidases are used, and 100:75:65 for high affinity oxidases. Our measured yields were 12, 8.5 and 6.7 $*10^{12}$ cells per mol electrons for the three pathways, i.e. a yield ratio of 100:71:56, which agrees reasonably with that predicted for low affinity oxidases.

The emerging evidence that bradyrhizobia with complete denitrification deplete N_2O in their surroundings before reducing available NO_3^- is promising from an environmental point of view since they have the potential to act as net sinks for N_2O produced by other organisms in their

499 vicinity. In legume fields, nodules and other N-rich organic material will be degraded, releasing
500 NH_4^+, which will rapidly be metabolized by nitrifying bacteria and archaea, producing NO_3^- while
501 consuming O_2. This will create optimal conditions for denitrification. Legume cropped fields
502 account for a significant share of the global N_2O emissions [5], and it is likely that coupled
503 nitrification-denitrification is a main cause [67]. One way of mitigating these emissions is to
504 enhance the number of efficient N_2O reducing bacteria in the soil microbial community. Rhizobial
505 inoculants are used since long to increase the yield of leguminous crops and at the same time
506 avoid the need for synthetic fertilizers. Different combinations of rhizobial strain and legume
507 cultivar may differ substantially in nitrogen fixation effectiveness, which is also affected by
508 environmental conditions [15, 68], and large efforts are put into the development of new
509 inoculants that are compatible with various types of legumes as well as soil types and climates
510 [69]. The present study shows that *Bradyrhizobium* strains also differ with respect to N_2O
511 reduction, and suggests that new inoculants should be selected among rhizobia that express Nos.

512

513 **Acknowledgements**

514 This project was supported by Kingenta Ecological Engineering Co., LTD. Yuan Gao is grateful to
515 the China Scholarship Council (CSC) for financial support. We thank Dr. Xinghua Sui from China
516 Agricultural University for providing seven of the *Bradyrhziobium* strains.

517

518 **References**

519 1. Rogelj J, Shindell D, Jiang K, Fifita S, Forster P, Ginzburg V et al. Mitigation pathways compatible
520 with 1.5 °C in the context of sustainable development. In, Masson-Delmotte V, Zhai P, Pörtner HO,
521 Roberts D, Skea J, Shukla PR, et al. (eds). *Global Warming of 1.5 °C. An IPCC Special Report on the*
522 *impacts of global warming of 1.5°C above pre-industrial levels and related global greenhouse gas*
523 *emission pathways, in the context of strengthening the global response to the threat ofclimate*
524 *change, sustainable development, and efforts to eradicate poverty*. 2018;
525 https://www.ipcc.ch/site/assets/uploads/sites/2/2019/02/SR15_Chapter2_Low_Res.pdf.
526 2. Thompson RL, Lassaletta L, Patra PK, Wilson C, Wells KC, Gressent A, et al. Acceleration of global

N_2O emissions seen from two decades of atmospheric inversion. *Nat Clim Chang* 2019; **9**: 993–998.

3. Thomson AJ, Giannopoulos G, Pretty J, Baggs EM, Richardson DJ. Biological sources and sinks of nitrous oxide and strategies to mitigate emissions. *Philos Trans R Soc B* 2012; **367**: 1157-1168.
4. Reay DS, Davidson EA, Smith KA, Smith P, Melillo JM, Dentener F, et al. Global agriculture and nitrous oxide emissions. *Nat Clim Chang* 2012; **2**: 410–416.
5. Jensen ES, Peoples MB, Boddey RM, Gresshoff PM, Hauggaard-Nielsen H, Alves JR, et al. Legumes for mitigation of climate change and the provision of feedstock for biofuels and biorefineries. A review. *Agron Sustain Dev* 2012; **32**: 329–364.
6. Schlesinger WH. On the fate of anthropogenic nitrogen. *Proc Natl Acad Sci* 2009; **106**: 203–208.
7. Davidson EA, Kanter D. Inventories and scenarios of nitrous oxide emissions. *Environ Res Lett* 2014; **9**: 105012.
8. Winiwarter W, Höglund-Isaksson L, Klimont Z, Schöpp W, Amann M. Technical opportunities to reduce global anthropogenic emissions of nitrous oxide. *Environ Res Lett* 2018; **13**: 014011.
9. Hénault C, Revellin C. Inoculants of leguminous crops for mitigating soil emissions of the greenhouse gas nitrous oxide. *Plant Soil* 2011; **346**: 289-296.
10. Itakura M, Uchida Y, Akiyama H, Hoshino YT, Shimomura Y, Morimoto S, et al. Mitigation of nitrous oxide emissions from soils by *Bradyrhizobium japonicum* inoculation. *Nat Clim Chang* 2013; **3**: 208–212.
11. Akiyama H, Hoshino YT, Itakura M, Shimomura Y, Wang Y, Yamamoto A, et al. Mitigation of soil N_2O emission by inoculation with a mixed culture of indigenous *Bradyrhizobium diazoefficiens*. *Sci Rep* 2016; **6**: 32869.
12. Zilli JÉ, Alves BJR, Rouws LFM, Simões-Araujo JL, de Barros Soares LH, Cassán F, et al. The importance of denitrification performed by nitrogen-fixing bacteria used as inoculants in South America. *Plant Soil* 2019; **451**: 5-24.
13. Obando M, Correa-Galeote D, Castellano-Hinojosa A, Gualpa J, Hidalgo A, Alché JD, et al. Analysis of the denitrification pathway and greenhouse gases emissions in *Bradyrhizobium* sp. strains used as biofertilizers in South America. *J Appl Microbiol* 2019; **127**: 739–749.
14. Thrall PH, Laine A-L, Broadhurst LM, Bagnall DJ, Brockwell J. Symbiotic effectiveness of rhizobial mutualists varies in interactions with native Australian legume genera. *PLoS ONE* 2011*;* **6**: e23545.
15. Woliy K, Degefu T, Frostegård Å. Host Range and Symbiotic Effectiveness of N_2O Reducing *Bradyrhizobium* Strains. *Front Microbiol* 2019; **10**: 2746.
16. Santos MS, Nogueira MA, Hungria M. Microbial inoculants: reviewing the past, discussing the

559 present and previewing an outstanding future for the use of beneficial bacteria in agriculture. *AMB*
560 *Expr* 2019; **9**: 205.
561 17. Arya SS, Salve AR, Chauhan S. Peanuts as functional food: a review. *J Food Sci Technol* 2016; **53**:
562 31–41.
563 18. Sameshima-Saito R, Chiba K, Minamisawa K. New method of denitrification analysis of
564 *Bradyrhizobium* field isolates by gas chromatographic determination of ^{15}N-labeled N_2. *Appl*
565 *Environ Microbiol* 2004; **70**: 2886–2891.
566 19. Mania D, Woliy K, Degefu T, Frostegård Å. A common mechanism for efficient N_2O reduction in
567 diverse isolates of nodule-forming bradyrhizobia. *Environ Microbiol* 2020; **22**: 17–31.
568 20. Sánchez C, Minamisawa K. Redundant roles of *Bradyrhizobium oligotrophicum* Cu-type (NirK) and
569 cd1-type (NirS) nitrite reductase genes under denitrifying conditions. *FEMS Microbiol Lett* 2018;
570 **365**: fny015.
571 21. Velasco L, Mesa S, Delgado MJ, Bedmar EJ. Characterization of the *nirK* gene encoding the
572 respiratory, Cu-containing nitrite reductase of *Bradyrhizobium japonicum*. *Biochim Biophys Acta*
573 2001; **1521**: 130–134.
574 22. Velasco L, Mesa S, Xu C, Delgado MJ, Bedmar EJ. Molecular characterization of *nosRZDFYLX* genes
575 coding for denitrifying nitrous oxide reductase of *Bradyrhizobium japonicum*. *Antonie Van*
576 *Leeuwenhoek* 2004; **85**: 229–235.
577 23. Mesa S, Velasco L, Manzanera ME, Delgado MJ, Bedmar EJ. Characterization of the *norCBQD* genes,
578 encoding nitric oxide reductase, in the nitrogen fixing bacterium *Bradyrhizobium japonicum*.
579 *Microbiology* 2002; **148**: 3553–3560.
580 24. Delgado MJ, Bonnard N, Tresierra-Ayala A, Bedmar EJ, Müller P. The *Bradyrhizobium japonicum*
581 *napEDABC* genes encoding the periplasmic nitrate reductase are essential for nitrate respiration.
582 *Microbiology* 2003; **149**: 3395–3403.
583 25. Bedmar EJ, Robles EF, Delgado MJ. The complete denitrification pathway of the symbiotic,
584 nitrogen-fixing bacterium *Bradyrhizobium japonicum*. *Biochem Soc Trans* 2005; **33**: 141–144.
585 26. Richardson DJ. Bacterial respiration: a flexible process for a changing environment. *Microbiology*
586 2000; **146**: 551–571.
587 27. Richardson DJ, Berks BC, Russell DA, Spiro S, Taylor CJ. Functional, biochemical and genetic
588 diversity of prokaryotic nitrate reductases. *Cell Mol Life Sci* 2001; **58**: 165–178.
589 28. Berks BC, Ferguson SJ, Moir JWB, Richardson DJ. Enzymes and associated electron transport
590 systems that catalyse the respiratory reduction of nitrogen oxides and oxyanions. *Biochim Biophys*

Acta 1995; **1232**: 97–173.

29. Zumft WG. Cell biology and molecular basis of denitrification. *Microbiol Mol Biol Rev* 1997; **61**: 533–616.
30. Zhang L, Wüst A, Prasser B, Müller C, Einsle O. Functional assembly of nitrous oxide reductase provides insights into copper site maturation. *Proc Natl Acad Sci* 2019; **116**: 12822–12827.
31. Zhang XP, Nick G, Kaijalainen S, Terefework Z, Paulin L, Tighe SW, et al. Phylogeny and Diversity of *Bradyrhizobium Strains* isoalted from the Root Nodules of Peanut *(Arachis hypogaea)* in Sichuan, China. *Syst Appl Microbiol* 1999; **22**: 378-386.
32. Van Rossum D, Muyotcha A, Van Verseveld HW, Stouthamer AH, Boogerd FC. Effects of *Bradyrhizobium* strain and host genotype, nodule dry weight and leaf aera on groundnut *(Arachis hypogaea L. ssp. fastigiata)* yield. *Plant and Soil* 1993; **154**: 279-288.
33. Van Rossum D, Muyotcha A, Van Verseveld HW, Stouthamer AH, Boogerd FC. Siderophore production by *Bradyrhizobium* spp. Strains nodulating groundnut. *Plant and soil* 1994; **163**: 177-187.
34. Chang YL, Wang ET, Sui XH, Zhang XX, Chen WX. Molecular diversity and phylogeny of rhizobia associated with *Lablab purpureus* (Linn.) grown in Southen China. *Syst Appl Microbiol* 2011; **34**: 276-284.
35. Wang R, Chang YL, Zheng WT, Zhang D, Zhang XX, Sui XH, et al. *Bradyrhizobium arachidis* sp. Nov., isolated from effective nodules of Arachis hypogaea grown in China *Syst Appl Microbiol 2013*; **36**: 101-105.
36. Li YH, Wang R, Zhang XX, Young PW, Wang ET, Sui XH, et al. *Bradyrhizobium guangdongense* sp. nov. and *Bradyrhizobium guangxiense* sp.nov., isolated from effectvie nodules of peanut. *Int J Syst Evol Microbiol* 2015; **65**: 4655-4661.
37. Degefu T, Wolde-meskel E, Woliy K, Frostegård Å. Phylogenetically diverse groups of *Bradyrhizobium* isolated from nodules of tree and annual legume species growing in Ethiopia. *Syst Appl Microbiol* 2017; **40**: 205-214.
38. Schwartz W, Vincent JM, a manual for the practical study of the root-nodule bacteria (IBP Handbuch no. 15 des international biology program, London). XI u. 164 S., 10 Abb., 17 tab., 7 Taf. Oxford-Edinburgh 1970: Blackwell scientific Publ.,45 s. *Z Allg Mikrobiol* 1972; 12: 1521–4028.
39. Molstad L, Dörsch P, Bakken LR. Robotized incubation system for monitoring gases (O_2, NO, N_2O N_2) in denitrifying cultures. *J Microbiol Methods* 2007; **71**: 202–211.
40. Sistrom WR. The kinetics of the synthesis of photopigments in Rhodopseudomonas spheroides. *J*

Gen Microbiol 1962; **28**: 607–616.

41. Bergaust L, Mao Y, Bakken LR, Frostegård Å. Denitrification response patterns during the transition to anoxic respiration and posttranscriptional effects of suboptimal ph on nitrogen oxide reductase in *Paracoccus denitrificans*. *Appl Environ Microbiol* 2010; **76**: 6387–6396.
42. Lycus P, Bøthun KL, Bergaust L, Shapleigh JP, Bakken LR, Frostegård Å. Phenotypic and genotypic richness of denitrifiers revealed by a novel isolation strategy. *ISME J* 2017; **11**: 2219–2232.
43. Molstad L, Dörsch P, Bakken LR. Improved robotized incubation system for gas kinetics in batch cultures. *ResearchGate* 2016; https://doi.org/10.13140/RG.2.2.30688.07680.
44. Cox RD. Determination of nitrate and nitrite at the parts per billion level by chemiluminescence. *Anal Chem* 1980; **52**: 332–335.
45. MacArthur PH, Shiva S, Gladwin MT. Measurement of circulating nitrite and S-nitrosothiols by reductive chemiluminescence. *J Chromatogr B* 2007; **851**: 93–105.
46. Larkin MA, Blackshields G, Brown NP, Chenna R, Mcgettigan PA, McWilliam H, et al. Clustal W and Clustal X version 2.0. *Bioinformatics* 2007; **23**: 2947–2948.
47. Hall TA. BioEdit: a user-friendly biological sequence alignment editor and analysis program for Windows 95/98/NT. *Nucleic Acids Symposium Series* 1999; **41***:* 95–98.
48. Kumar S, Stecher G, Tamura K. MEGA7: Molecular Evolutionary Genetics Analysis Version 7.0 for Bigger Datasets. *Mol Biol Evol* 2016; **33**: 1870–1874.
49. Ronquist F, Teslenko M, Van Der Mark P, Ayres DL, Darling A, Höhna S, et al. Mrbayes 3.2: Efficient bayesian phylogenetic inference and model choice across a large model space. *Syst Biol* 2012; **61**: 539–542.
50. Rambaut A, Drummond AJ, Xie D, Baele G, Suchard MA. Posterior summarization in Bayesian phylogenetics using Tracer 1.7. *Syst Biol* 2018; **67**: 901–904.
51. Chaumeil PA, Mussig AJ, Hugenholtz P, Parks DH. GTDB-Tk: a toolkit to classify genomes with the Genome Taxonomy Database. *Bioinformatics* 2020; 36: 1925-1927.
52. Conthe M, Lycus P, Arntzen MØ, Ramos da Silva A, Frostegård Å, Bakken LR, et al. Denitrification as an N_2O sink. *Water Res* 2019; **151**: 381–387.
53. Avontuur JR, Palmer M, Beukes CW, Chan WY, Coetzee MPA, Blom J, et al. Genome-informed *Bradyrhizobium* taxonomy: where to from here? *Syst Appl Microbiol* 2019; **42**: 427-439.
54. Delmont TO, Prestat E, Keegan KP, Faubladier M, Robe P, Clark IM, et al. Structure, fluctuation and magnitude of a natural grassland soil metagenome. *ISME J* 2012; **6**: 1677-1687.
55. Xu ZF, Hansen MA, Hansen LH, Jacquiod S, Sørensen SJ. Bioinformatic Approaches Reveal

655 Metagenomic Characterization of Soil Microbial Community. *PLoS ONE* 2014; **9**: e93445.
656 56. Lycus P, Soriano-Laguna MJ, Kjos M, Richardson DJ, Gates AJ, Milligan DA, et al. A bet-hedging
657 strategy for denitrifying bacteria curtails their release of N_2O. *Proc Natl Acad Sci* 2018; **115**: 11820–
658 11825.
659 57. Torres MJ, Simon J, Rowley G, Bedmar EJ, Richardson DJ, Gates AJ, et al. Nitrous oxide metabolism
660 in nitrate-reducing bacteria: physiology and regulatory mechanisms. In: Poole RK (eds). *Advances in*
661 *microbial physiology*, first edition. Elsevier, 2016; pp 353-432.
662 58. Liu B, Mao Y, Bergaust L, Bakken LR, Frostegård Å. Strains in the genus *Thauera* exhibit remarkably
663 different denitrification regulatory phenotypes. *Environ Microbiol* 2013; **15**: 2816–2828.
664 59. Gaimster H, Hews CL, Griffiths R, Soriano-Laguna MJ, Alston M, Richardson DJ, et al. A central small
665 RNA regulatory circuit controlling bacterial denitrification and N_2O emissions. *mBio* 2019; **10**:
666 e01165-19.
667 60. Jiménez-Leiva A, Cabrera JJ, Bueno E, Torres MJ, Salazar S, Bedmar EJ, et al. Expanding the Regulon
668 of the *Bradyrhizobium diazoefficiens* NnrR Transcription Factor: New Insights Into the
669 Denitrification Pathway. *Front Microbiol* 2019; **10**: 1926.
670 61. Shapleigh JP. The prokaryotes: Prokaryotic physiology and biochemistry. In Rosenberg E, DeLong
671 EF, Lory S, Stackebrandt E, Thompson F (eds). *The prokaryotes.* Springer: Berlin Heidelberg, 2013;
672 pp 405–425.
673 62. Bueno E, Robles EF, Torres MJ, Krell T, Bedmar EJ, Delgado MJ, et al. Disparate response to
674 microoxia and nitrogen oxides of the *Bradyrhizobium japonicum napEDABC*, *nirK* and *norCBQD*
675 denitrification genes. *Nitric Oxide* 2017; **68**: 137–149.
676 63. Torres MJ, Bueno E, Jiménez-Leiva A, Cabrera JJ, Bedmar EJ, Mesa S, et al. $FixK_2$ Is the Main
677 Transcriptional Activator of *Bradyrhizobium diazoefficiens nosRZDYFLX* Genes in Response to Low
678 Oxygen. *Front Microbiol* 2017; **8**: 1621.
679 64. Falk S, Liu B, Braker G. Isolation, genetic and functional characterization of novel soil *nirK*-type
680 denitrifiers. *Syst Appl Microbiol* 2010; **33**: 337–347.
681 65. Casella S, Shapleigh JP, Toffanin A, Basaglia M. Investigation into the role of the truncated
682 denitrification chain in *Rhizobium sullae* strain HCNT1. *Biochem Soc Trans* 2006; **34**: 130-132.
683 66. Van Spanning R, Richardson D, Ferguson S. Introduction to the biochemistry and molecular biology
684 of denitrification. In: Bothe H,Ferguson SJ, Newton WE (eds). *Biology of the nitrogen cylce*. Elsevier:
685 Amsterdam, The Netherlands, 2007; pp 3–21.
686 67. Bakken LR, Frostegård Å. Sources and sinks for N_2O, can microbiologist help to mitigate N_2O

687 emissions? *Environ Microbiol* 2017; **19**: 4801-4805.

688 68. Lindström K, Mousavi SA. Effectiveness of nitrogen fixation in rhizobia. *Microb. Biotechnol.* 2019;

689 https://doi.org/10.1111/1751-7915.13517.

690 69. Martínez J, Negrete-Yankelevich S, Godinez LG, Reyes J, Esposti MD, Martínez Romero E. Short-

691 Term Evolution of Rhizobial Strains Toward Sustainability in Agriculture. In *Microbial Models: From*

692 *Environmental to Industrial Sustainability*. Springer: Singapore, 2016; pp. 277–292.

693

694

695

Table 1 Strains used in the current study. Strains AC 70c, AC 86d2, AC 86j1 and AC 101b (below dashed line) were included in the phylogenetic analysis in the present study but were not examined for denitrification since this was reported elsewhere [19].

Strain	Host plant	Geographic origin	Reference
HAMBI 2115*	*Arachis hypogaea* L.	Zimbabwe	[31]
HAMBI 2116	*A. hypogaea* L.	Zimbabwe	[31]
HAMBI 2125	*A. hypogaea* L.	Sichuan, China	[31]
HAMBI 2127	*A. hypogaea* L.	Sichuan, China	[31]
HAMBI 2128	*Macrotyloma africanum*	Zimbabwe	[32]
HAMBI 2130	*Vigna unguiculata*	Zimbabwe	[33]
HAMBI 2134	*A. hypogaea* L.	Sichuan, China	[31]
HAMBI 2142	*A. hypogaea* L.	Sichuan, China	[31]
HAMBI 2149	*A. hypogaea* L.	Sichuan, China	[31]
HAMBI 2153	*A. hypogaea* L.	Israel	[31]
HAMBI 2299	*A. hypogaea* L.	Hawaii, USA	HAMBI**
HAMBI 3052^{T}	*Lablab purpureus*	Anhui, China	[34]
CCBAU 051107^{T}	*A. hypogaea* L.	Hebei, China	[35]
CCBAU 23155	*A. hypogaea* L.	Anhui, China	[35]
CCBAU 33067	*A. hypogaea* L.	Jiangxi, China	[35]
CCBAU 45332	*A. hypogaea* L.	Henan, China	[35]
CCBAU 53344	*A. hypogaea* L.	Guangxi, China	[36]
CCBAU 53363^{T}	*A. hypogaea* L.	Guangxi, China	[36]
CCBAU 53429	*A. hypogaea* L.	Guangxi, China	[36]
AC70c	*Phaseolus vulgaris*	Akaki, Ethiopia	[37]
AC86d2	*Cajanus cajan*	Awassa, Ethiopia	[37]
AC87j	*Millettia ferruginea*	Awassa, Ethiopia	[37]
AC101b	*Acacia saligna*	Leku, Ethiopia	[37]

HAMBI: The culture collection at the Department of Microbiology, University of Helsinki.
CCBAU: Culture Collection of China Agricultural University, Beijing, China.
AC: The strains are kept in a local collection at Norwegian University of Life Sciences and available upon request (Å. Frostegård).
*) For information on donator and specimen history of HAMBI strains please consult https://kotka.luomus.fi/culture/bac
**) https://kotka.luomus.fi/view?uri=http://tun.fi/RAH.1747&type=document&page=1&spot=1

Table 2 Denitrification gene operons of *Bradyrhizobium* strains, analyzed based on whole genome sequencing. Strains placed within the same section of the table were highly similar as seen from pairwise genome comparison, with ANI values >99.2, and in most cases >99.9 % (Table S4). They also had the same denitrification phenotype. Strains representing each of these clusters are marked in bold and were included in the phylogenetic tree (Fig. 1). Presence (+) or absence (-) of functional and regulatory/accessory genes are indicated. Colors represent a function detected after analysis of denitrification end products (blue= nitrate reduction; yellow = nitrite reduction; red = nitric oxide reduction; and green = nitrous oxide reduction). Blank = absence of function. The amino acid sequences of the *nor* operons of strains HAMBI 2299 and HAMBI 2153 were compared to those of the strains listed here (in bold) that produced functional reductases (except strain CCBAU 53363^T).

Bradyrhizobium strains	Nitrate reduction					Nitrite reduction		Nitric oxide reduction					Nitrous oxide reduction						
	nap					***nir***		***nor***					***nos***						
	E	*D*	*A*	*B*	*C*	*K*	*V*	*C*	*B*	*Q*	*D*	*E*	*R*	*Z*	*D*	*Y*	*F*	*L*	*X*
HAMBI 2125 HAMBI 2126	+	+	+	+	+	+	+	+	+	+	+	+	+	+	+	+	+	+	+
HAMBI 2127	+	+	+	+	+	+	+	+	+	+	+	+	+	+	+	+	+	+	+
HAMBI 2130	+	+	+	+	+	+	+	+	+	+	+	+	+	+	+	+	+	+	+
HAMBI 3052^T	+	+	+	+	+	+	+	+	+	+	+	+	+	+	+	+	+	+	+
***CCBAU 53363^T**	+	+	+	+	+	+	+	+	+	+	+	+	+	+	+	+	+	+	+
HAMBI 2115	+	+	+	+	+	+	+	+	+	+	+	+	-	-	-	-	-	-	-
HAMBI 2116	+	+	+	+	+	+	+	+	+	+	+	+	-	-	-	-	-	-	-
HAMBI 2128 HAMBI 2129 HAMBI 2150	+	+	+	+	+	+	+	+	+	+	+	+	-	-	-	-	-	-	-
HAMBI 2134 HAMBI 2135	+	+	+	+	+	+	+	+	+	+	+	+	-	-	-	-	-	-	-
HAMBI 2142	+	+	+	+	+	+	+	+	+	+	+	+	-	-	-	-	-	-	-
****HAMBI 2153**	+	+	+	+	+	+	+	+	-	-	+	+	-	-	-	-	-	-	-
HAMBI 2299	+	+	+	+	+	+	+	+	+	+	+	+	-	-	-	-	-	-	-
HAMBI 2149 HAMBI 2133 HAMBI 2136 HAMBI 2137 HAMBI 2151 HAMBI 2152	+	+	+	+	+	+	+	-	-	-	-	-	-	-	-	-	-	-	-

*The accession number for the complete genome sequence of CCBAU 53363 in NCBI is CP022219.

** A frame shift in *norB*; *norQ* is not in the correct reading frame.

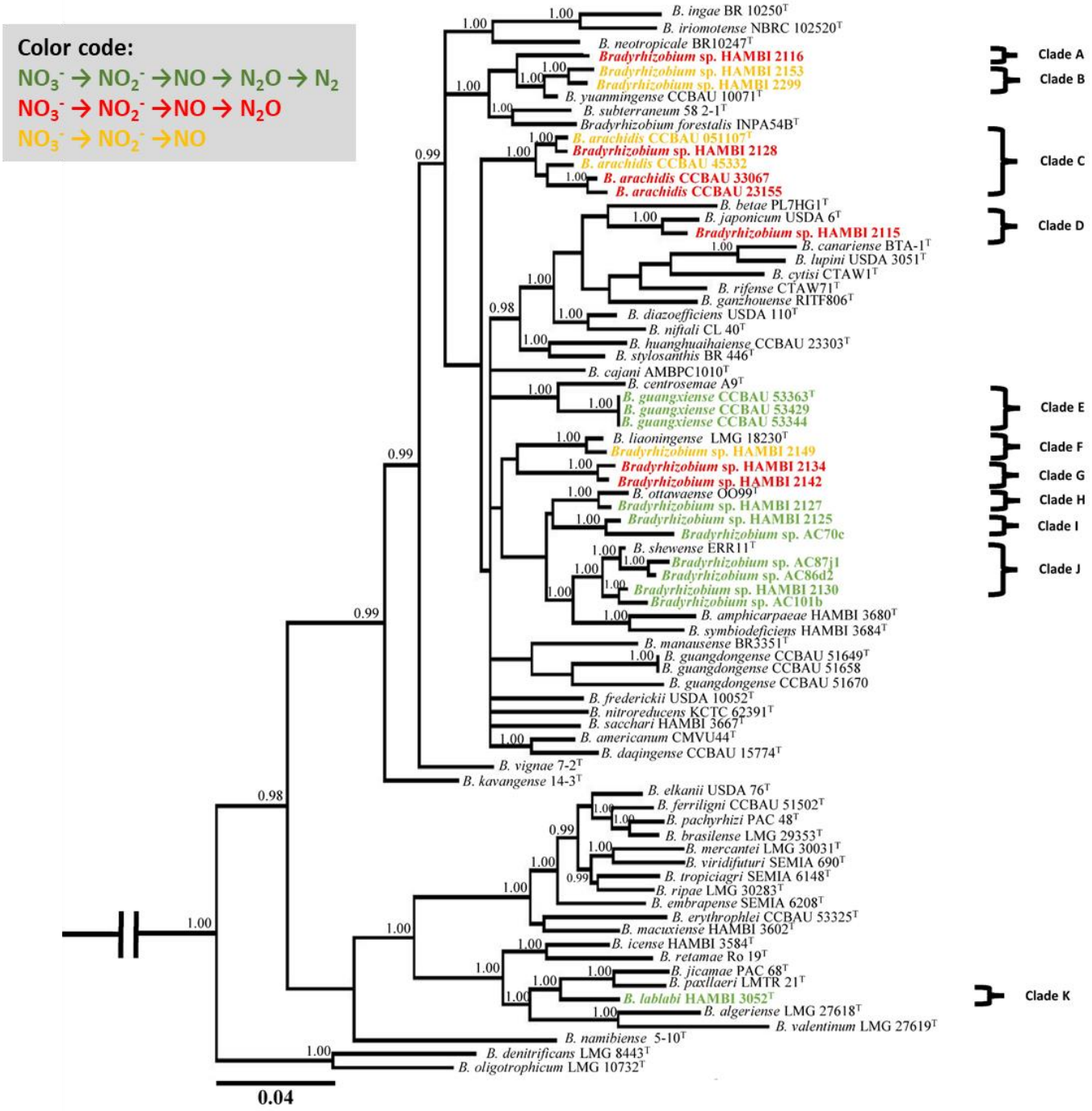

Fig. 1 Phylogenetic tree of four concatenated housekeeping genes (*atpD- glnII- recA- rpoB*) from 78 bradyrhizobial strains constructed based on a Bayesian inference analysis. Only the posterior probabilities ≥0.95 are shown in the tree. The genus name *Bradyrhizobium* is abbreviated as *B.*, and a "T" at the end of each strain code shows the type strains. Colors indicate denitrification end-products, determined in this study, except for strains AC87ji, AC 86d2, AC 70c and AC 101b which were reported by [19].

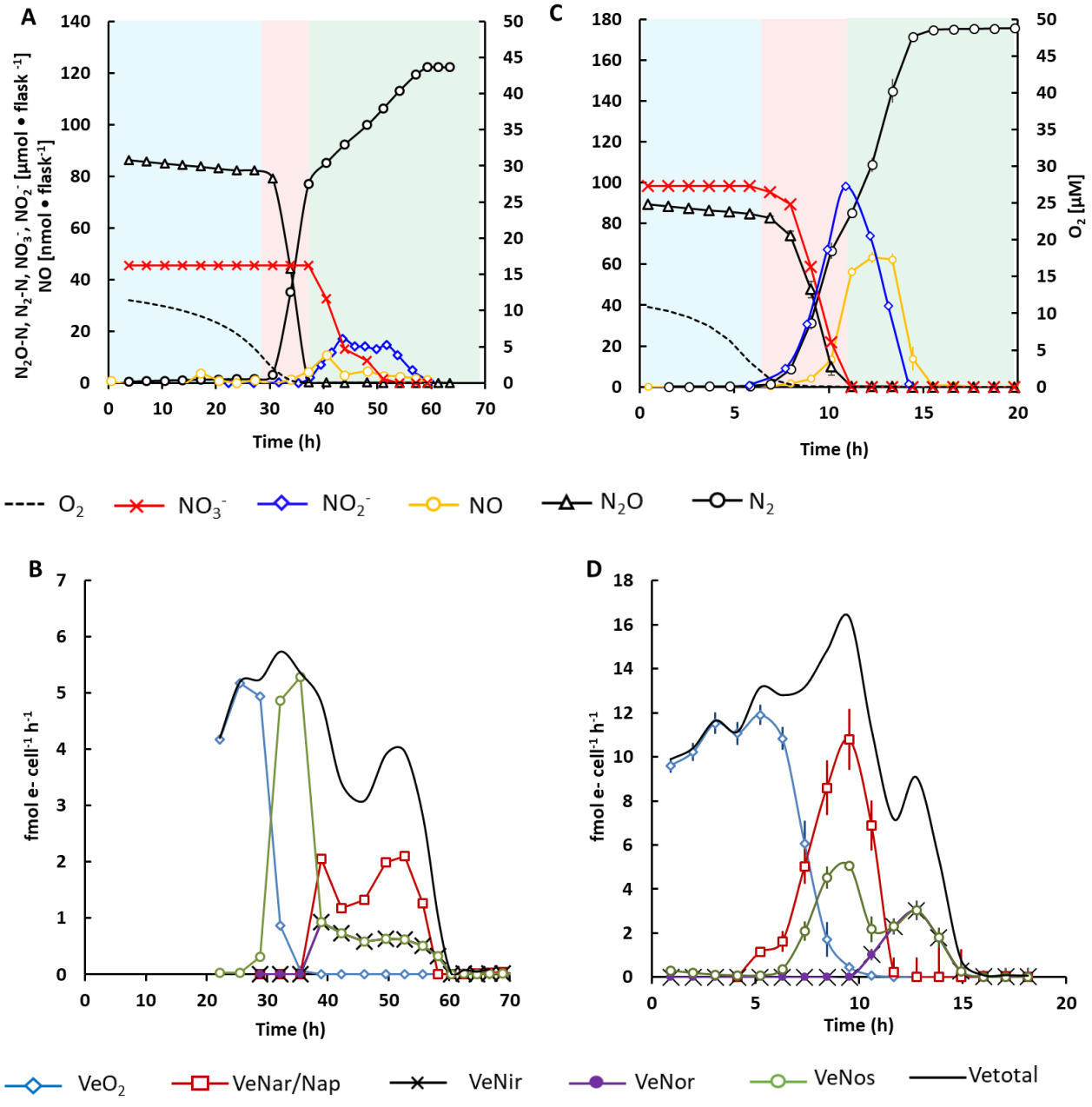

Fig. 2 Competition for electrons between N_2O- and NO_3^- reductase; comparison of Nap- and Nar-carrying organisms. Comparison of gas kinetics and corresponding electron flow to oxidases (aerobic respiration) and the different N-reductases measured in batch cultures of *Bradyrhizobium* strain HAMBI 2125, which carries Nap and Nos but lacks Nar (A and B) and *Paracoccus denitrificans* which carries Nap, Nar and Nos (C and D). The top panels (A & C) show the measured amounts of NO_2^-, NO, N_2O and N_2 per vial, and the concentration of O_2 in the liquid. Note that the small but significant decrease in N_2O during the aerobic phase was caused by sampling losses, not by N_2O reduction or other reactions, as explained in Fig. S9. The The bottom panels show the calculated cell specific rates of electron flow (fmol $cell^{-1}$ h^{-1}) to the terminal oxidases (V_{eO2}) and to the four reductases ($V_{eNar/Nap}$, V_{eNir}, V_{eNor} and V_{eNos}). V_{eNir} and

V_{eNor} were practically identical throughout (NO remained very low), thus indistinguishable in the panels. Strain HAMBI 2125 was incubated in 4 replicate flasks with YMB supplemented with 1 mM KNO_3, of which only one is shown here (replicate vials are shown in Fig. S3). *P. denitrificans* was incubated in 50 ml Sistrom's medium with 2 mM KNO_3 (n=7 replicate vials, standard error indicated by vertical lines). At the start of the incubation, all vials contained ~1% O_2 in the headspace (~10 µM in liquid) and ~ 1.2 ml N_2O (~90 µmol N_2O-N). $V_{eNar/Nap}$ and V_{eNir} in legend (B and D) represents rate of electron transport to NO_3^- and NO_2^-, respectively (via NapA and NirK for *Bradyrhziobium* and NarG+Nap and NirS for *P. denitrificans*).

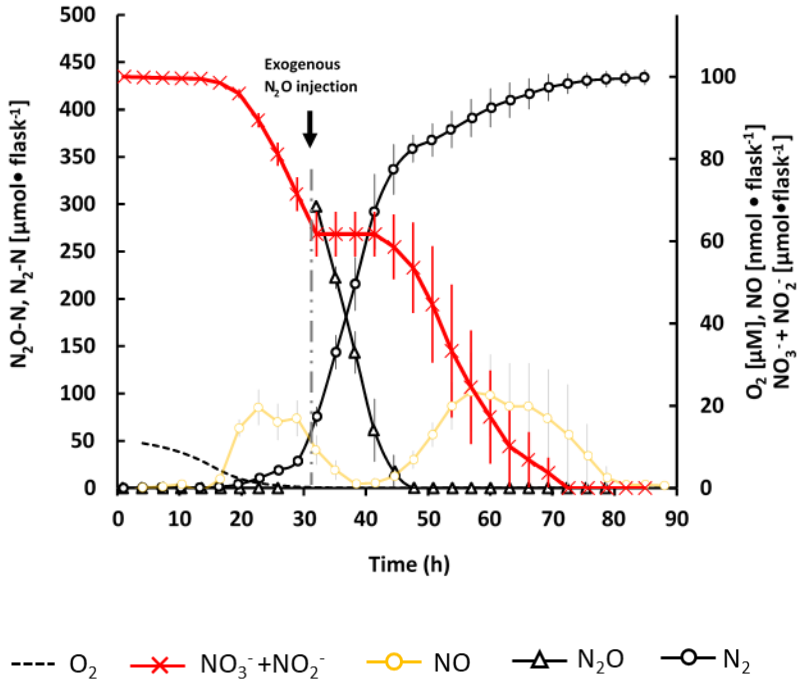

Fig. 3 Effect of injecting N_2O to an actively denitrifying culture. Gas kinetics for *Bradyrhizobium* strain HAMBI 2125 during and after transition from aerobic respiration to N-oxide respiration. Triplicate cultures were incubated in YMB medium supplemented with 2 mM KNO_3 and with 0.7 ml O_2 in the headspace (around 10 µM O_2 in the medium). Approximately 4 ml N_2O (~300 µmol N_2O-N) were injected at 32 hpi, indicated by the arrow, into actively denitrifying cultures respiring NO_3^-. Bars show standard errors (n=3).

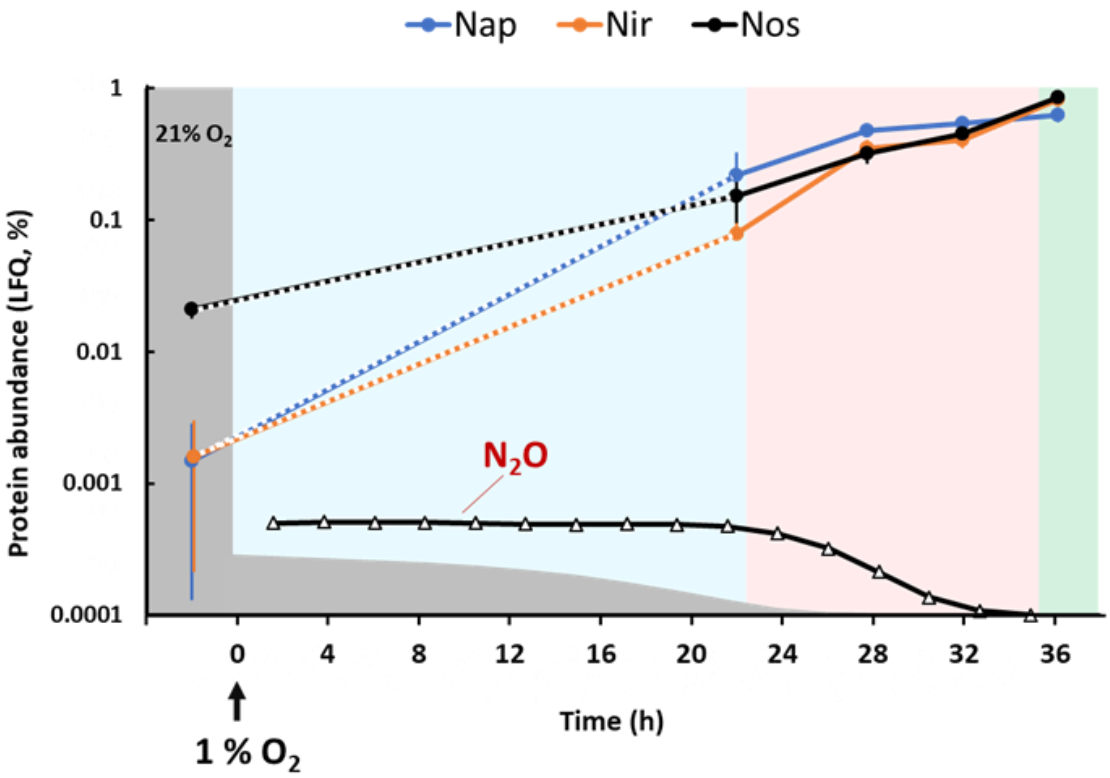

Fig. 4 Quantification of denitrifying reductase molecules throughout transition from aerobic to anaerobic respiration. The panel shows the concentrations of Nap, Nir and Nos determined by proteomics analysis together with the concentration of O_2 and N_2O. The abundance of the individual denitrification reductases were calculated as percentages of the sum of all LFQ (label-free quantitation of proteins) abundances for each time point. The first samples were taken from triplicate vials of aerobically grown of *Bradyrhizobium* strain HAMBI 2125 growing under fully aerobic conditions (21% O_2). The precultures were used to inoculate vials with 1% O_2, which were sampled when reaching hypoxia, and during the subsequent anoxic respiration. The amounts of O_2 and N_2O are indicated to illustrate the time of their depletion, and the colors indicate 4 distinct phases: 1) fully oxic (gray), 2) transition to hypoxic conditions (blue), 3) early anoxic with respiration based on N_2O-reduction and 4) anoxic with respiration by NO_3 reduction (green). For actual values of [O_2] [N_2O], [N_2] and [NO_2^-], see Fig. S6. Bars show standard deviation (n=3).